Vol.02, Issue 03 (2024): 20-27
DOI: 10.58921/jse.02.03.062

Journal of Sustainable Environment
ISSN (p): 2710-2386, ISSN (e): 2957-9228

Published by
1885 SMI UNIVERSITY

Utilization of Azadirachta Indica Latex for Synthesis of Silver Nanoparticles its Application in Photocatalytic Degradation of Methylene Blue Dye

Ambreen Shahadat[1*], Waqar Ahmed[1], Urooj Haroon[2] , Khalid Ahmed[3]

[1] Institute of Environmental Studies, University of Karachi, Karachi, Pakistan

[2] Department of Chemistry, Federal Urdu University Arts, Science and Technology, Karachi, Pakistan

[3] L. E. J. Nanotechnology Centre, H. E. J. Research Institute of Chemistry, International Centre for Chemical and Biological Sciences, University of Karachi, Karachi, 75270, Pakistan

Corresponding Author: gabrielambreen@gmail.com

ABSTRACT

The use of extract from indigenous plant species for the synthesis of metallic nanoparticles has significant importance as they have a capacity to act as potential reducing, capping and stabilizing agent. In this research, latex of *Azadirachta indica* (Neem) was selected for green synthesis of silver nanoparticles (AgNPs). Maximum absorbance was achieved at 425 nm (λ_{max}) for AgNPs. FTIR vibrational peaks of AgNPs were observed at 3462, 2933, 1732, 1658, 1458, 1381, 1244, and 1028 and near 600 cm $^{-1}$. Moreover, Atomic Force Microscopy (AFM) showed that the synthesized AgNPs were face-centered cuboid, spherical, hexahedral, and pentagonal structures ranging in size between 7.15-71.5nm. XRD analysis shows that most of the nanoparticles have spherical crystalline structure. Photocatalytic degradation of hazardous azo dye; Methylene blue dye (MB) was performed in the presence of synthesized AgNPs as catalysts under UV-induced photocatalytic degradation. The degradation efficiency after 180 minutes of reaction time was 82 % which proposes its potential to use as environmental pollutant eradicators in the treatment of textile industries wastewater.

Keywords *Azadirachta indica, Nanoparticles, FTIR, Photocatalytic Degradation, Azo Dye.*

1. INTRODUCTION

Currently, technological development and rapid industrialization have caused massive environmental deterioration due to which future generations are going to face serious consequences of environmental pollution (Hussain, 2015). Recently, remarkable advancements in nanotechnology have drawn researcher's attention towards sustainable production and its application. Several conventional (Chemical / biological) methods are widely used for the synthesis of metallic nanoparticles. However, these methods required noxious and expensive chemicals. Therefore, it identifies a research gap to propose an alternative method for the synthesis of nanoparticles. For that greener approach for the synthesis of nanoparticles has gained prime focus of researchers as they are more stable, require less reaction time, cost-effective, do not need hazardous chemicals and can be tailored to obtain particles of desired shape and size (Iravani, 2011). Plants or their exudates such as roots, shoots, bark, fruits, leaves, and seeds possess a variety of biomolecules and metabolites such as vitamins, proteins, polyphenols, alkaloids, sugars, steroids, flavonoids (quercetin and isoquercetin), fatty acids (oleic and linoleic), tannic acids, glycosides, terpenoids etc, which contains carboxylic, hydroxyl, carbonyl, and amino groups that may be used as reducing, capping or stabilizing agents (Makarov et al., 2014: Valsalam et al., 2019: Singh et al., 2021). Biogenic metal nanoparticles are easier to synthesize and one of their unique characteristics is a high surface-to-volume ratio which increases the reactivity of nanomaterials. Gold (Au), Cobalt (Co), silver (Ag), platinum (Pt), Zinc (Zn), Ferric (Fe), and Palladium (Pd) are some of the most researched metallic nanoparticles (Aritonang et al., 2019). The morphology of synthesized nanoparticles is also controlled by other factors like pH, temperature, time, concentration of metal salt and type of biological extracts used (Jadoun et al., 2021). Literature survey revealed that AgNPs have been synthesized by various plant extracts such as skin and gel of *Aloe vera (*Hashoosh et al., 2014), latex and leaf extract obtained from *Jatropha curcas* (Ogbogo et al., 2022; Kumar et al., 2017) *Emblica officinalis* (Amla*)* (Ramesh et al., 2015) *Cinnamomum camphora*, fruit extract of *Musa balbisiana* (Banana), *Carica papaya* leaf extract (Banala et al., 2015), *Crataegus douglasii* (Li, et al., 2021) and by various other plant extracts (Banerjee et al., 2014; Giri et al., 2022).

Azadirachta indica, an ever-green native plant member of the mahogany family, Meliaceae is widely spread in the tropical and sub-tropical regions. Different aerial parts including leaves, bark, flowers, fruit, gum, and oil are associated with the medical folklore from ancient times (Islas et al., 2020). The white milky juice of this plant is rich in biomolecules and is not much studied in synthesis of nanomaterials that could be utilized in different applications such as catalytic activity, optical properties, chemical sensing, biological imaging, electronic properties, gene silencing, drug delivery, antimicrobial and magnetic properties and more specifically environmental remediation due to simple method and stability (Abou El-Nour et al., 2010; Zhang et al., 2016).

The journal is hosted and maintained by smiu.edu.pk .Works are licensed under CC BY-SA

Textile industry effluent transports different dyes into aquatic ecosystems that causing critical destruction to micro and macro-organisms, disturbance in photosynthesis activities and decreased level of dissolved oxygen (DO) in water (Cruz et al., 2019). Most of the dyes are carcinogenic and their aromatic structure makes them stable and difficult to degrade (Alizadeh et al., 2017).

In the last few decades, different physical and chemical processes such as, adsorption, oxidation, reduction and decomposition have been developed and applied to minimize the pollutant load. These processes have huge energy demand, high cost, require hazardous chemicals and involve complicated reactions (Anastopoulos et al., 2018). The development of sustainable, ecofriendly, and cost-effective methods is much needed for the degradation of dyes in wastewater. Hence, adopting greener synthesis techniques for metal nanoparticles stands as a crucial method imperative to address this issue. Accordingly, this research reports a greener synthesis of AgNPs and their photocatalytic degradation potential to degrade commonly used heterocyclic aromatic cation structure azo dye Methylene Blue (MB) often used in textile industries. *Azadirachta indica* (Neem) Latex was chosen for the present study as a biogenic agent for synthesizing AgNPs, since this plant is quite commonly available in our surroundings, and it can minimize the addition of hazardous external stabilizing and capping agents during synthesis.

Figure 1: Azadirachta indica (Neem) Tree and its Latex

2. MATERIALS AND METHODS

2.1 Materials

From Sigma Aldrich Chemical Company, Karachi, Pakistan $AgNO_3$, NaOH and other relevant chemicals were purchased. Fresh latex of *Azadirachta indica* was extracted and filtered through double fold muslin cloth and proceeded for AgNPs synthesis.

2.2 Qualitative Phytochemical Analysis of Azadirachta indica Latex

The latex of *Azadirachta indica* was screened and identified their bioactive constituents. These phytoconstituents were examined by standard methods (Mahendiran et al., 2017; Aziz et al., 2020; Akila et al., 2016; Hameed et al., 2018).

2.3 Synthesis of Silver nanoparticles (AgNPs)

Green synthesis for AgNPs was used according to the modified procedure (Al aboody, 2019). 3% of aqueous solution of latex extract of *Azadirachta indica* was prepared by diluting 3 mL of latex in 100 mL of DI water. In 90 mL of diluted latex extract, 1.0 mM silver nitrate ($AgNO_3$) solution used as precursor and was added drop wise with constant stirring at room temperature in dark to avoid unnecessary photochemical reaction. The total reaction time for the completion of reaction is 24h. A significant change in the color of solution was observed from white to dark brown representing bio-reduction of Ag^+ to Ag^o. The obtained AgNPs were settled at the bottom, when centrifuge at 20.000 rpm for 15 minutes. Theses NPs were vortexed and then washed with DI water (n = 3) to remove excessive biological material.

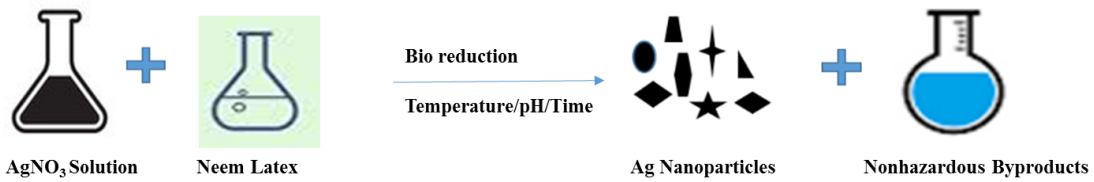

Figure 2: Reaction Mechanism of AgNPs synthesis using Neem Latex
(Kuppusamy et al., 2014)

2.4 Characterization of AgNPs

Bioreduction of Ag^+ was initially characterized by UV-visible spectroscopy (BK-UV1800, Biobase China). The particles were scanned from 300-700 nm and absorbance was recorded at a fixed wavelength (λ_{max}). The morphology was performed by Atomic Force Microscopy (AFM-5500 Agilent Technologies) and Energy Dispersive X-ray spectrum (EDX) for crystalline nature identification. Fourier Transform Infrared Spectroscopy

(FTIR) was performed by Thermo Scientific ™ FTIR spectrophotometer (BRUKER, Vector-22) to analyze the functional groups in biomolecules present in the latex of *Azadirachta indica* over the range of 4000 – 400 cm^{-1}. To resolve the size, shape and surface morphology of synthesized AgNPs Scanning Electron Microscopy (SEM, JSM IT100 Japan) was used.

2.5 Photocatalytic Degradation of Dyes

For photocatalytic degradation study of MB dye using synthesized AgNPs under ultraviolet (UV) irradiation adsorption method was performed under controlled conditions in laboratory. According to Sing et. al. 3 mL solution of MB dye (1 mM) was mixed with 3 mL of DI water and 2 mL of AgNPs, to make a total volume of up to 8 mL (Singh et.al, 2021). The solution was then placed in a black box with an 11-Watt UV lamp. The catalytic degradation efficiency was calculated in triplicate (n = 3) based on absorbance reading. A control solution (without AgNPs) was also set up for comparison (n = 1). For 20 minutes, the mixture was stirred in dark to build up the adsorption-desorption equilibrium then exposed to UV light under constant stirring at room temperature for 90 minutes. The degradation efficiencies were calculated according to the following equation:

$$D\ (\%) = \frac{C_o - C_f}{C_o} * 100$$

Where C_o = initial concentration of dye (mgL^{-1}) at t = 0 minute and C_f = final residual concentration at the end of adsorption time directly measured after 15 minutes of exposure for 90 minutes. To measure the color intensity Absorbance was observed by UV-vis spectrophotometer.

3. RESULTS & DISCUSSION

3.1 Phytochemical Analysis of Plant Latex

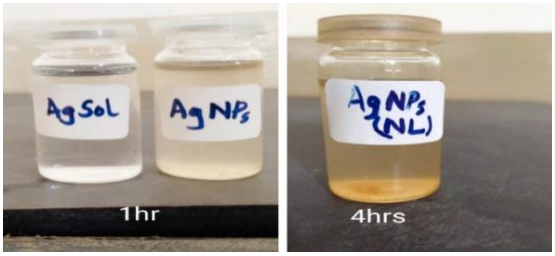

Figure 3: Color change indicates formation of AgNPs

General screening of neem latex exhibited the presence of Tannins, Alkaloids, Flavonoids, Saponins, Steroids and polyphenolic compounds as mentioned in table 1. These compounds react with $AgNO_3$ to synthesize AgNPs. The white milky solution turns brown as shown in figure 3.

Table 1: Phytochemical Screening of Neem Latex

Phytochemicals Components	Alkaloids	Flavonoids	Saponine		Phenols	Tannins	Steroids	Carbohydrates	Glycosides		Terpenoides	Quinones	Anthraquinone
			Frothing	Emulsion					Cardic	Cyanogenic			
Interferences	++	++	+	+	++	++	++	+	**ND**	**ND**	**ND**	**ND**	**ND**
Strongly Present (++), Present (+), Not Detected (ND)													

3.2 UV-Visible Absorbance Spectra of AgNPs

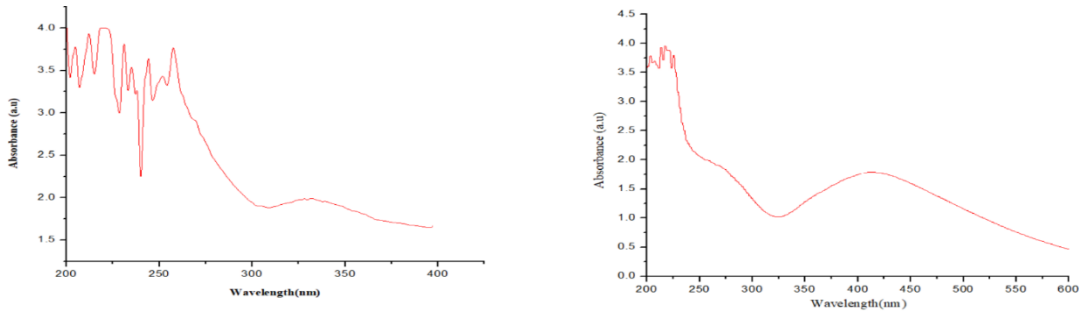

Figure 4: UV-visible spectra of Azadirachta Indica Latex and Silver Nanoparticles

AgNPs formation was detected using UV-vis analysis. The absorbance spectrum of latex in Figure 4 shows an absorption peak around 325 nm (Figure 4) indicates the presence if unsaturated bonds of oxygen, sulfur, and nitrogen (Njokua et al., 2013). However, it is difficult to match peaks to specific elements or functional group in a complex systems and analysis through UV alone cannot completely identify it. Therefore, more additional analysis other than UV alone is recommended for understandable characterization of (Karpagasundari & Kulothungan, 2014). Figure 4 shows a strong broad peak at 425 nm due to surface plasmon resonance. Ashraf et.al. describes the UV-visible spectrum of AgNPs in the range of 400 - 500 nm (Ashraf et al., 2016).

3.3 FT-IR Spectral Analysis of AgNPs

FTIR of AgNPs was studied to determine the various functional groups present in neem latex and predict their role in the synthesis. The FTIR spectrum illustrates absorption bands at 3462, 2933, 1732, 1658, 1458, 1381, 1244, and 1028 and near 600cm^{-1}. A broad and strong absorbance peak at 3462cm^{-1} corresponds to O–H vibration, arising from phenolic compounds or carboxylic groups in the extract. The observed peak at 2933cm^{-1} represents vibration of aromatic (C-H stretch) while peak at 1732 corresponds to C=O absorption. Peaks at 1658 and 1458 are assigned to the C=C stretching vibrations of the aromatic rings. Peak at 1381 cm^{-1} demonstrates the N–O symmetry stretching, which represents nitro compound while absorption bands at 1244 and 1028 correspond to the C-N and C-O stretch. The presence of C=O, C-N and C-O absorption indicates the existence of amides and proteins in the extract. The absorption peak at 600 cm^{-1} could be due to the presence of alkyl halides (C–Br) (Okaiyeto et al., 2021; Jain et al., 2021). Appearance of new absorption bands at 3755, 2860 and 2378cm^{-1} and shift in peaks position and intensity in the IR spectrum of AgNPs is attributed to their involvement in the stability and/or capping of AgNPs, reported in many research studies. Moreover, absorption bands at 1732 cm^{-1} and 600 cm^{-1} nearly diminished in the AgNPs FT-IR spectrum possibly due to the stabilization of AgNPs through these sites (Yazdi et al., 2019).

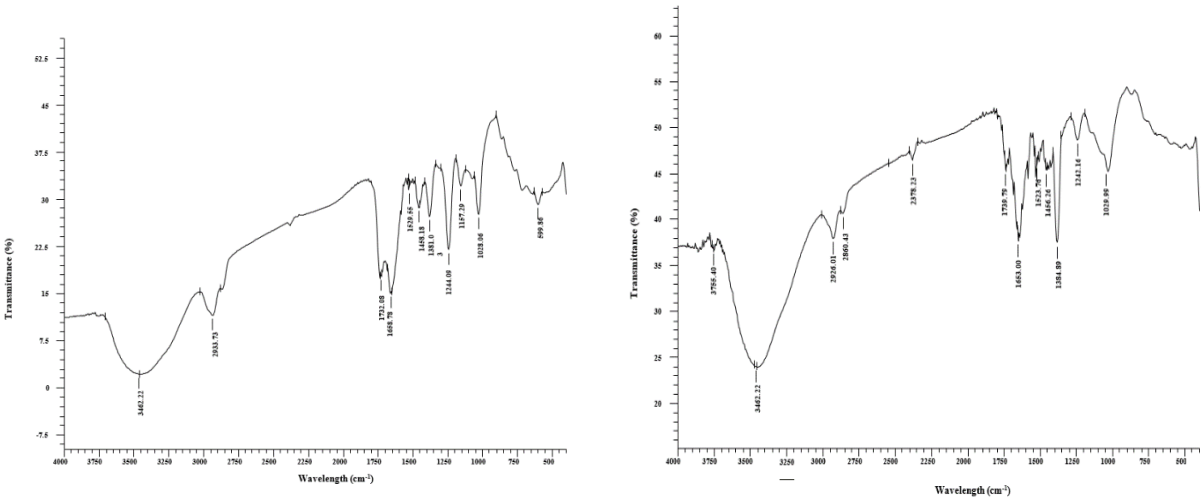

Figure 5. FTIR Spectra of AgNPs synthesized by Neem Latex

3.4 XRD Structural Analysis

The crystalline nature and phase composition of AgNPs were identified with a Bragg angle X-ray diffractometer in the range from 0° to 80° within 2θ range, with a fine focus Cu tube (λ = 1.54 Å).

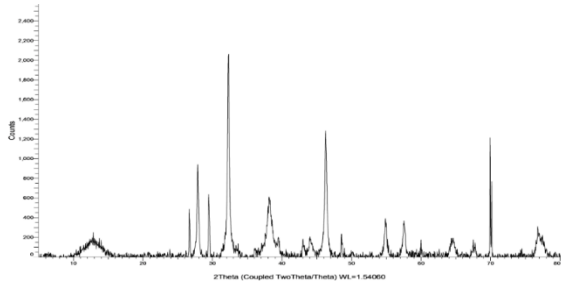

Figure 6. XRD Patterns of AgNPs

XRD pattern of silver nanoparticles using neem latex is shown in Figure 6. XRD data show diffraction peaks at 2θ shows several broad Bragg peaks corresponding to 38.2°, 44.4°, 64.6°, and 77.5° and can be indexed to 111, 200, 220, 311 and 222 orientations, respectively indicating the crystalline nature of AgNPs. Results confirmed that AgNPs formed by the reduction of Ag^+ ions by the neem latex were essentially crystalline and are consistent

with earlier reports (Kumar et al., 2013). The intensity of AgNPs of (200) and (220) diffraction were much stronger than others. The unassigned peaks were considered to be crystalline and amorphous organic phases.

3.4 Atomic Force Microscopy Analysis (AFM)

The surface morphology of the AgNPs synthesized from Azadirachta indica neem latex was characterized using Atomic Force Microscopy. A 2.54 x 2.54µm region was scanned to obtain an image and estimate the surface features and 3D topography. **Figure 7** AFM image reveals that the AgNPs exhibit a spherical, hexahedral and pentagons shape with an average size of around ~ 7.15-71.5nm.

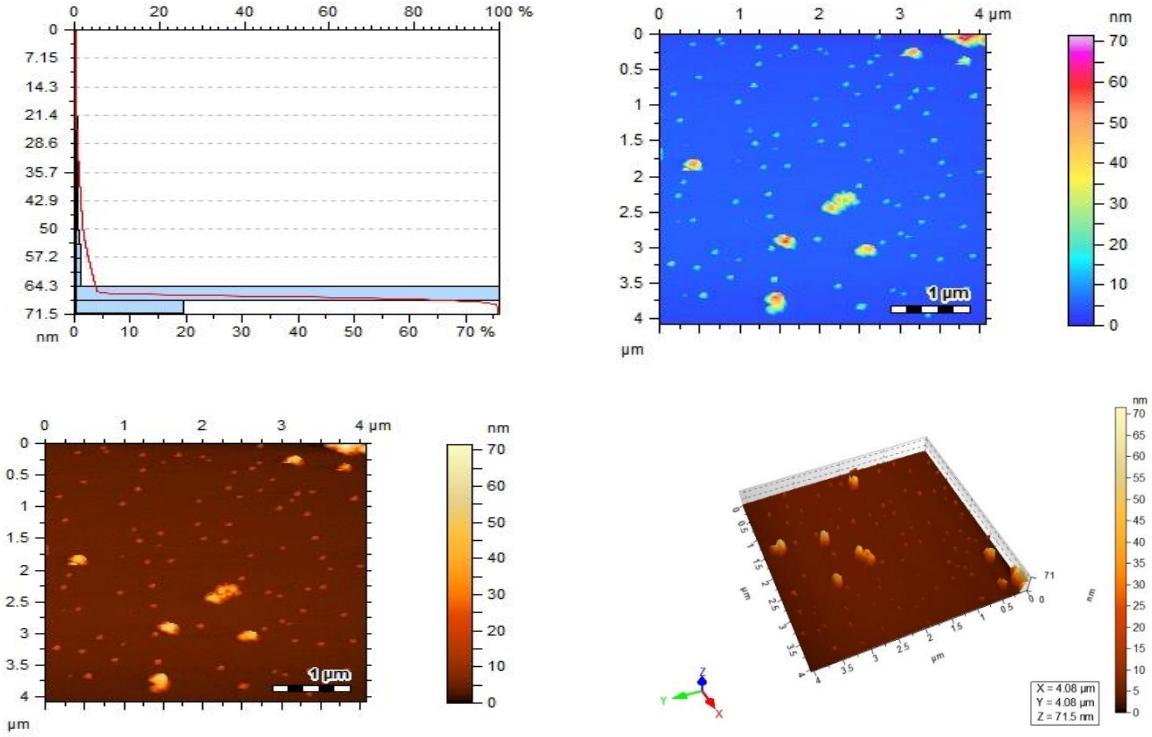

Figure 7. AFM images showing spherical, hexahedral and pentagonal structures of AgNPs

3.5 Scanning Electron Microscopy (SEM)

To understand the morphology and shape or size of AgNPs, SEM was used in this study. Figure 9 shows the size ranging between 37 to 76 nm of latex-based AgNPs having triangles, pentagons, hexagons and cuboid structure and their size ranged between 37-76 nm in diameter.

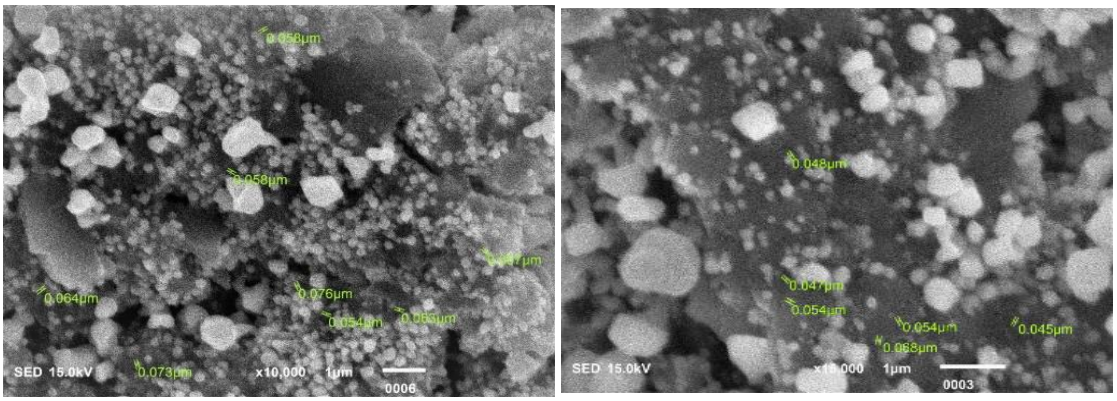

Figure 9. SEM images of AgNPs using Latex of Azardica Indica

Synthesized nanoparticles were found to be highly scattered due to electrostatic reflection. Further, it could also be seen that few particles size 5 – 10 nm were linked to the surface of large particles (Banerjee et al., 2014).

3.6 EDX Pattern

According to Jyoti et. al. (Jyoti et al., 2016) due to surface plasmon resonance the AgNPs exhibits a typical peak at 3KeV. Figure 8 shows sharp peaks between 3 and 4 KeV in the EDX patterns of AgNPs confirming the presence of silver similar to Memon et.al. reported in literature (Memon et. al 2017). The reduction of silver ion to silver metal (Ag^+ to Ag) indicated by high peak of silver while a weak oxygen peak has been originated.

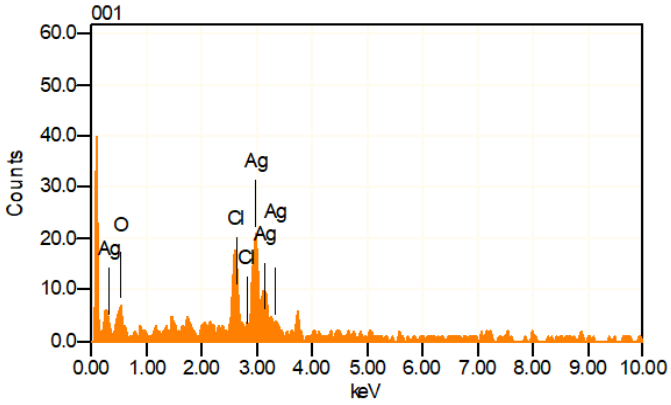

Figure 8. EDX Patterns of AgNPs

3.7 Photocatalytic Degradation of Methylene Blue (MB)

For the photocatalytic activity, under UV light irradiation aqueous solution of MB dye was studied using biosynthesized AgNPs as photocatalyst. Figure 10a. shows the degradation of UV-visible spectra of MB dye at different times with intervals of 30 minutes. (0, 30, 60, 90, 120, 150 and 180 minutes). At absorption maxima of MB dye (665 nm) shows significant reduction in absorption after UV light irradiation in the first 30 minutes, then gradual decrease was observed in the absorbance with 15 minutes time interval to 180 minutes. The percent degrading efficiency (D%) of AgNPs was plotted as a function of time (Figure 10b). MB dye was observed degraded to AgNPs in the presence of UV light as 0, 38.3%, 45.7%, 56.1%, 66.14%, 74.8%, and 85.3% at 0, 30, 60, 90, 120, 150 and180 minutes respectively. At the end of the irradiation of 180 minutes, MB dye was degraded to 85% of its initial value with a visible color change from dark blue to very light blue as depicted in figure 10c. Degradation of MB solution shows gradual color change. This research provides sufficient knowledge and proof of the usage of AgNPs as efficient and powerful agent for environmental remediation applications.

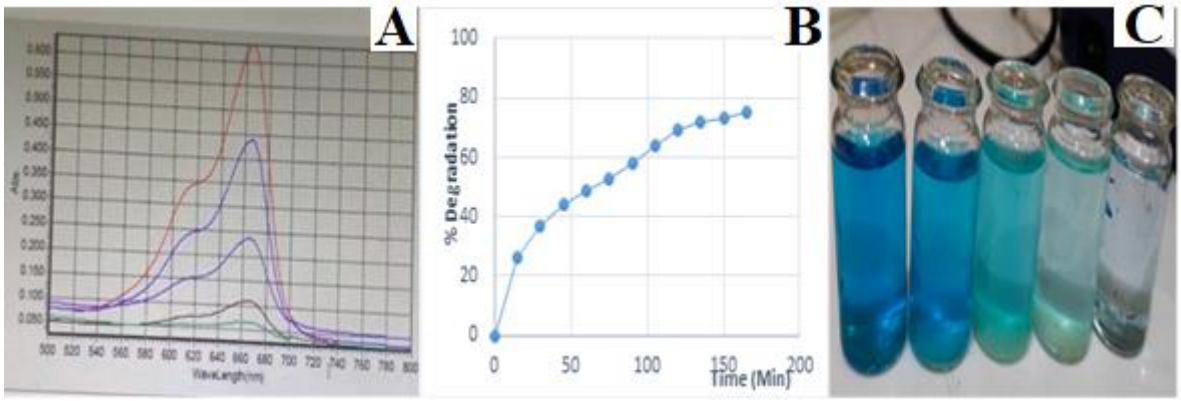

Figure 9: A) Photocatalytic degradation of MB dye. B) % Degradation with Time. C) MB color changes

4. CONCLUSION

In this study, a simple, ecofriendly, and low-cost method has been developed to synthesize Ag nanoparticles via a biogenic method using neem latex. The synthesis of particles was confirmed by UV and IR spectrophotometry with SEM revealing an average particle size of 37-76 nm. Moreover, the size of nanoparticles decreased when pH of the reaction cell is increased. The size and crystallinity of particles were confirmed by XRD pattern. Through AFM average dimension of AgNPs was confirmed and found in agreement with XRD results which is 64.3 nm. The synthesized nanomaterial effectively demonstrated photocatalytic activity to degrade MB dye offering novel approach for the community to create low cost, ecofriendly photocatalyst technique for effective removal of dye from wastewater.

5. REFERENCES

Abou El-Nour, K. M., Eftaiha, A. A., Al-Warthan, A., & Ammar, R. A. (2010). Synthesis and applications of silver nanoparticles. Arabian journal of chemistry, 3(3), 135-140.

Akila, P., Prince, L., Bharathidasan, R., & Krishnapriya, K. (2016). Antibacterial activity of herbal plants. *Int. J. Curr. Microbiol. Appl. Sci*, *5*, 681-688.

Al Aboody, M. S. (2019). Silver/silver chloride (Ag/AgCl) nanoparticles synthesized from Azadirachta indica lalex and its antibiofilm activity against fluconazole resistant Candida tropicalis. *Artificial Cells, Nanomedicine, and Biotechnology*, *47*(1), 2107-2113.

Anastopoulos, I., Hosseini-Bandegharaei, A., Fu, J., Mitropoulos, A. C., & Kyzas, G. Z. (2018). Use of nanoparticles for dye adsorption. Journal of Dispersion Science and Technology, 39(6), 836-847.

Aritonang, H. F., Koleangan, H., & Wuntu, A. D. (2019). Synthesis of silver nanoparticles using aqueous extract of medicinal plants'(Impatiens balsamina and Lantana camara) fresh leaves and analysis of antimicrobial activity. *International journal of Microbiology*, *2019*.

Aziz, F., Taqdees, M., Ifrah, I., & Sayyada, G. N. (2020). Phytochemical screening and antibacterial activity of neem extracts on uropathogens. Pure Appl. Biol., 9 (1): 148-153.

Banala, R. R., Nagati, V. B., & Karnati, P. R. (2015). Green synthesis and characterization of Carica papaya leaf extract coated silver nanoparticles through X-ray diffraction, electron microscopy and evaluation of bactericidal properties. Saudi Journal of Biological Sciences, 22(5), 637-644.

Banerjee, P., Satapathy, M., Mukhopahayay, A., & Das, P. (2014). Leaf extract mediated green synthesis of silver nanoparticles from widely available Indian plants: synthesis, characterization, antimicrobial property and toxicity analysis. *Bioresources and Bioprocessing*, *1*(1), 1-10.

Cruz, J. C., Nascimento, M. A., Amaral, H. A., Lima, D. S., Teixeira, A. P. C., & Lopes, R. P. (2019). Synthesis and characterization of cobalt nanoparticles for application in the removal of textile dye. Journal of environmental management, 242, 220-228.

Giri, A. K., Jena, B., Biswal, B., Pradhan, A. K., Arakha, M., Acharya, S., & Acharya, L. (2022). Green synthesis and characterization of silver nanoparticles using Eugenia roxburghii DC. extract and activity against biofilm-producing bacteria. *Scientific Reports*, *12*(1), 1-9.

Hameed, A.S., Saatam, H. R., Thamir, H., Kadhum, M. H., Al Roomi, R., & Hussain T, Al. Isam. (2018). Production of iron nanoparticle by using Aloe vera gel and studying its effect on Lepidium sativum seed germination. *International Journal of Biosciences, 13(4): 248-255*.

Hashoosh, S. I., Fadhil, A. M., & Al-Ani, N. K. (2014). Production of Ag nanoparticles using Aloe vera extract and its antimicrobial activity. Al-Nahrain Journal of Science, 17(2), 165-171.

Hudlikar, M., Joglekar, S., Dhaygude, M., & Kodam, K. (2012). Latex-mediated synthesis of ZnS nanoparticles: green synthesis approach. *Journal of Nanoparticle Research*, *14*(5), 1-6.

Hussain, I., Singh, N. B., Singh, A., Singh, H., & Singh, S. C. (2016). Green synthesis of nanoparticles and its potential application. *Biotechnology letters*, *38*(4), 545-560.

Iravani, S. (2011). Green synthesis of metal nanoparticles using plants. *Green Chemistry*, *13*(10), 2638-2650.

Islas, J. F., Acosta, E., Zuca, G., Delgado-Gallegos, J. L., Moreno-Treviño, M. G., Escalante, B., & Moreno-Cuevas, J. E. (2020). An overview of Neem (Azadirachta indica) and its potential impact on health. *Journal of Functional Foods*, *74*, 104171.

Jadoun, S., Arif, R., Jangid, N. K., & Meena, R. K. (2021). Green synthesis of nanoparticles using plant extracts: A review. *Environmental Chemistry Letters*, *19*(1), 355-374.

Jain, N., Jain, P., Rajput, D., & Patil, U. K. (2021). Green synthesized plant-based silver nanoparticles: Therapeutic prospective for anticancer and antiviral activity. Micro and Nano Systems Letters, 9(1), 5.

Kumar, S., Bhattacharya, W., Singh, M., Halder, D., & Mitra, A. (2017). Plant latex capped colloidal silver nanoparticles: A potent anti-biofilm and fungicidal formulation. Journal of Molecular Liquids, 230, 705-713.

Kumari, O. S., & Rao, N. B. (2015). Phyto chemical analysis of piper betel leaf extract. World Journal of Pharmacy and Pharmaceutical Sciences (WJPPS), 4(1), 699-703.

Kuppusamy, P., Yusoff, M. M., Maniam, G. P., & Govindan, N. (2016). Biosynthesis of metallic nanoparticles using plant derivatives and their new avenues in pharmacological applications–An updated report. *Saudi Pharmaceutical Journal*, *24*(4), 473-484.

Li, W., Qu, F., Chen, Y., Sun, Y., Zhang, J., Xie, G., ... & Xu, H. (2021). Antimicrobial activity of sliver nanoparticles synthesized by the leaf extract of Cinnamomum camphora. Biochemical Engineering Journal, 172, 108050.

Mahendiran, D., Subash, G., Arumai Selvan, D., Rehana, D., Senthil Kumar, R., & Kalilur Rahiman, A. (2017). Biosynthesis of zinc oxide nanoparticles using plant extracts of Aloe vera and Hibiscus sabdariffa: phytochemical, antibacterial, antioxidant and anti-proliferative studies. *BioNanoScience*, *7*(3), 530-545.

Makarov, V. V., Love, A. J., Sinitsyna, O. V., Makarova, S. S., Yaminsky, I. V., Taliansky, M. E., & Kalinina, N. O. (2014). "Green" nanotechnologies: synthesis of metal nanoparticles using plants. *Acta Naturae (англоязычная версия)*, *6*(1 (20), 35-44.

Menon, S., Agarwal, H., Kumar, S. R., & Kumar, S. V. (2017). Green synthesis of silver nanoparticles using medicinal plant Acalypha indica leaf extracts and its application as an antioxidant and antimicrobial agent against foodborne pathogens. Int. J. Appl. Pharm, 9, 42-50.

Ogbogo, I. O., Ikyenge, B. A., Ishwah, B., Weor, T. T., & Adoga, S. O. (2022). Synthesis, Characterization and Antibacterial Activity Studies of Eco-Friendly Silver Nanoparticles from the Leaf Extract of Jatropha Curcas. Sch Int J Chem Mater Sci, 5(8), 128-134.

Okaiyeto, K., Hoppe, H., & Okoh, A. I. (2021). Plant-based synthesis of silver nanoparticles using aqueous leaf extract of Salvia officinalis: characterization and its antiplasmodial activity. Journal of Cluster Science, 32, 101-109.

Ramesh, P. S., Kokila, T., & Geetha, D. (2015). Plant mediated green synthesis and antibacterial activity of silver nanoparticles using Emblica officinalis fruit extract. Spectrochimica Acta Part A: Molecular and Biomolecular Spectroscopy, 142, 339-343.

Singh, I., Gupta, S., Gautam, H. K., Dhawan, G., & Kumar, P. (2021). Antimicrobial, radical scavenging, and dye degradation potential of nontoxic biogenic silver nanoparticles using Cassia fistula pods. *Chemical Papers*, *75*(3), 979-991.

Valsalam, S., Agastian, P., Arasu, M. V., Al-Dhabi, N. A., Ghilan, A. K. M., Kaviyarasu, K., ... & Arokiyaraj, S. (2019). Rapid biosynthesis and characterization of silver nanoparticles from the leaf extract of Tropaeolum majus L. and its enhanced in-vitro antibacterial, antifungal, antioxidant and anticancer properties. *Journal of Photochemistry and Photobiology B: Biology*, *191*, 65-74.

Yazdi, M. E. T., Amiri, M. S., Hosseini, H. A., Oskuee, R. K., Mosawee, H., Pakravanan, K., & Darroudi, M. (2019). Plant-based synthesis of silver nanoparticles in Handelia trichophylla and their biological activities. Bulletin of Materials Science, 42(4), 155.

Zhang, X. F., Liu, Z. G., Shen, W., & Gurunathan, S. (2016). Silver nanoparticles: synthesis, characterization, properties, applications, and therapeutic approaches. International journal of molecular sciences, 17(9), 1534.